Punching Shear Behavior of Reinforced Concrete Isolated Footings Reinforced with GFRP Rebars

Sothea Som[1] and Supakorn Tirapat[1,*]

[1]Sustainable Infrastructure Research and Development Center, Department of Civil Engineering, Faculty of Engineering, Khon Kaen University, Khon Kaen 40002, Thailand

**Corresponding author; E-mail address: supati@kkumail.com*

Abstract

The punching shear strength of isolated footings varies considerably for different codes, partly due to varying amounts of soil reaction considered when calculating the punching shear resistance. The present study aimed to investigate the punching shear behavior of reinforced concrete isolated footings reinforced with GFRP rebars, taking into account soil-structure interaction. Full-scale specimens were divided into two groups based on the type of foundation support and were tested separately. One group was supported on a bed of elastic springs to simulate an elastic foundation based on Winkler-type soil reactions, while the other was supported on a rigid support to examine the effect of soil-structure interaction on the punching shear behavior. The specimens were tested to investigate the load-carrying capacity, failure mode, subgrade reaction, crack development, footing slab deflection, and rebar strain distribution. Results from the tests showed that the elastic spring system maintained a constant k value despite the vertical settlement. Both tested specimens failed in punching shear failure mode, and the specimen supported by the elastic spring system had a little higher punching shear resistance than the one supported on a rigid support. Additionally, the resistance of the specimens exceeded the calculated value according to the ACI code, suggests that the code is reliable and perhaps more conservative.

Keywords: Punching Shear, GFRP Rebar, Footing, Reinforced Concrete, Elastic Foundation

1. Introduction

Reinforced concrete structures have gained widespread popularity due to their strength, durability, and comparatively low construction cost when compared to other types of structures. However, the corrosion of steel reinforcement within these structures has emerged as a significant concern in the modern construction industry [1]. The corrosion of steel reinforcement bars in reinforced concrete structures exposed to harsh marine environments is caused by chloride ions, which can reduce the load-carrying capacity of the elements by decreasing the diameter of the corroded bars and affecting their flexural and bond strength. Researchers have suggested various solutions, including using different types of steel reinforcing bars and improving concrete quality. However, the high cost of repairing corrosion damage has led to the development of a new reinforcing material, FRP bars, which have high strength and corrosion resistance and can replace steel reinforcement in reinforced concrete structures. Using FRP bars in reinforced concrete footings, which are in direct contact with soil and difficult to repair, is particularly important for improving the performance of the structures and avoiding expensive repair cost.

To transfer the weight of a structure to the ground, footings resting on soil are used. However, the pressure of the soil beneath the footings depends on the type and stiffness of the soil, making it difficult to predict the behavior of the footings. Additionally, if concrete footings fail due to punching shear, it can cause the entire structure to collapse in a brittle manner [2,3]. Consequently, researchers have conducted numerous experiments and theoretical studies to understand the punching-shear behavior of concrete-column footings.

Hegger et al. [4,5], Siburg and Hegger [6], Bonić and Folić [7], and Bonić et al. [8] conducted punching shear tests on RC footings using real sand. While Kevi et al. [9], Oskouei et al. [10], and Saleh et al. [11] investigated the punching behavior of GFRP footings on real soil support. The test result shows that the capacity and shear crack in footings is affected by the a/d ratio.

Shear reinforcement can enhance punching capacity, while concrete strength has a greater influence than the reinforcement ratio. GFRP-reinforced concrete footings have lower capacity and wider cracks compared to steel-reinforced footings.

Talbot [12], Lee et al. [13], and Truong et al. [14] performed punching shear tests on RC footing and ground slab using elastic springs to simulate an elastic foundation based on Winkler-type soil reactions. According to the test results, the elastic spring system was consistent throughout the test, and the test participants' behavior on it was comparable to the other support systems.

For this present study, the punching shear behavior of reinforced concrete isolated footings reinforced with GFRP rebars considering soil-structure interaction was investigated. In this study, an elastic steel spring system that simulates the elastic foundation based on Winkler-type soil reactions was used to support the test specimen compared with a rigid support. Moreover, the test results were compared with the punching shear resistance predictions from the ACI code.

2. Experimental program

2.1 Test specimens

In this study, two square footings with a square stub column were constructed. The size of the tested footings was chosen to be approximately equal to the size of common footings usually used in residential buildings. Both specimens had the same dimensions of 1,000 x 1,000 x 200 mm, with a square stub column prepared at the center of the footing with dimensions of 150 x 150 x 150 mm. The main reinforcement consisted of 4 DB20 mm (SD40T) steel bars, and 4 RB9 mm (SR24) steel bars stirrups were used as transverse reinforcement for both specimens. All tested footings had the same reinforcement ratio of 0.62% and the same concrete compressive strength of 25 MPa. The specimens were divided into two groups: the first group (F1) was supported by a bed of elastic springs to simulate an elastic foundation based on Winkler-type soil reactions, while the other (F2) was supported by a rigid support to examine the effect of soil-structure interaction. Table 1 and Fig. 1 provide full details of the tested specimens.

Table 1 Summary of experimental program

Footing ID	l (mm)	b (mm)	h (mm)	d (mm)	Φ (mm)	ρ (%)	Support
F1	1,000	1,000	200	150	13	0.62	Spring
F2	1,000	1,000	200	150	13	0.62	Rigid

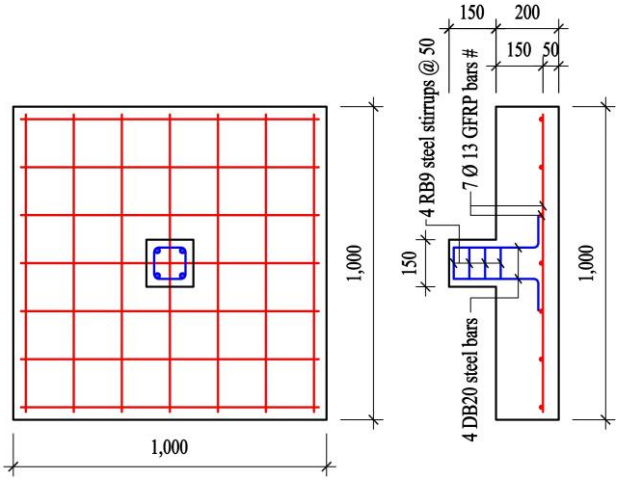

Fig. 1 Dimensions and detail of specimens F1, and F2 (Unit: mm)

2.2 Material properties

2.2.1 Reinforcement bars

The tested footing specimens were reinforced with ribbed bars of Glass Fiber Reinforced Polymer (GFRP bars) that were 13 mm in diameter and met the Thai Industrial Standards (TIS. 2973-2562) [15]. To determine the ultimate tensile strength, ultimate strain, and modulus of elasticity of the bars, GFRP bar specimens were tested following ASTM D7205/D7205M-06 [16]. The measured ultimate tensile strength, ultimate strain, and modulus of elasticity of GFRP bars with 13 mm diameter were 942 MPa, 0.021, and 45,187 MPa, respectively. The steel ribbed bars and round steel bars, supplied according to the Thai Industrial Standards SD40T (TIS. 24-2559) [17] and SR24 (TIS. 20-2559) [18], respectively were used for stub columns.

2.2.2 Concrete

For all tested specimens, commercial-ready mixed concrete was used. The concrete mixture was designed to reach a standard cylinder sample (Φ150x300 mm) strength of approximately $f_c^{'} =$ 25 MPa on the day of testing. To assess the strength of the standard cylindrical samples, ASTM C39/C39M-14 [19] was followed.

2.3 Test setup

A hydraulic actuator with a capacity of 2,000 kN was used to apply a concentrated axial load through a stub column to each isolated footing. The test setup of the isolated footing tests is shown in Fig. 4 and Fig. 5. To support the reaction forces from the hydraulic actuator, a robust main steel frame was built on a sturdy floor.

To simulate an elastic foundation based on Winkler-type soil reactions, the F1 specimen was tested while being supported by nine elastic springs. Each of these steel springs has dimensions of 45 mm in diameter, 200 mm in outer diameter, and 620 mm in height. The modulus of soil reaction was estimated to be 0.010 N/mm^3, which represents the medium-dense sand [20]. Within the elastic limit of deformation of 186 mm, the spring stiffness remains constant at 1.074 kN/mm.

In accordance with Fig. 3, the F2 specimen was tested using supporting beams that has a clear span of 750 mm in both directions.

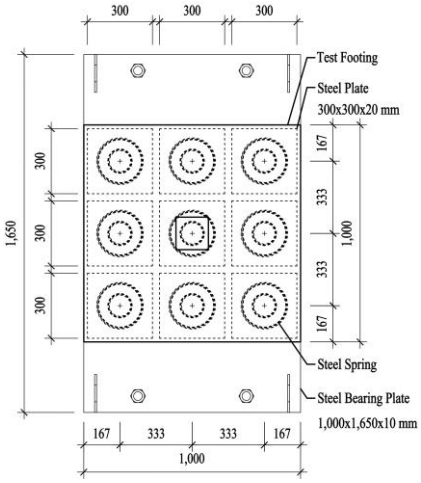

(a) Plane

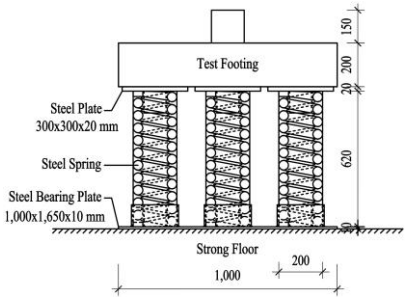

(b) Elevation

Fig. 2 Elastic spring system (Unit: mm)

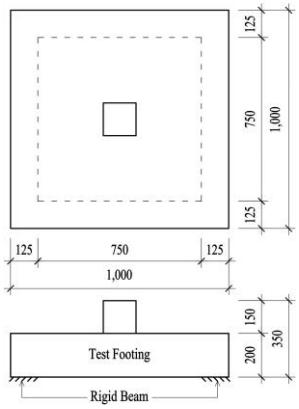

Fig. 3 Rigid support (Unit: mm)

Fig. 4 Test setup on the elastic spring system

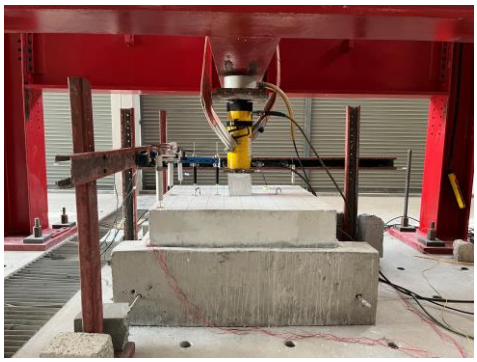

Fig. 5 Test setup on the rigid support

2.4 Measurement instrumentations

For both tested footings, nine LVDTs with an accuracy of 0.01 mm were used to measure the footing displacement. The positions of transducers are shown in Fig. 6. At nine locations, D1 to D9 displacement transducers were placed in both directions on top of the footing. Strain measurements on longitudinal reinforcing GFRP were taken at different locations as shown in Fig. 7. All strain gauges were placed on the undersurface of the reinforcement, with “B” and “T” referring to the bottom layer and top layer, respectively. The strain gauges were all made by KYOWA, type KFGS-2-120-C1-11 L5M2R for reinforcement bar with a gauge length is 2 mm and 120.4Ω ± 0.4% gage resistance. The strain gauges B1, B2, B3, T1, T2, and T3 were bonded to the GFRP bars.

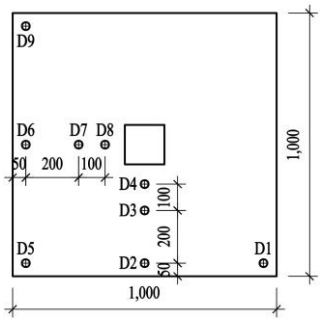

Fig. 6 Layout of displacement measurement (Unit: mm)

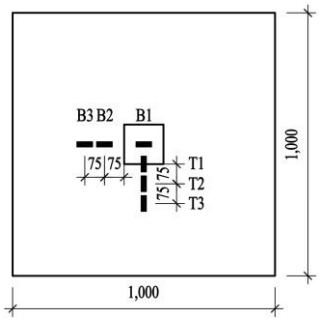

Fig. 7 Layout of rebar strain gages (Unit: mm)

3. Test results

3.1 Mode of failure, crack pattern, and failure load

Both tested footings failed due to punching shear with no signs of flexural failure observed. The crack pattern at the end of the testing is depicted in Fig. 8 and Fig. 9.

Fig. 8 Bottom surface crack patterns at failure of F1

Fig. 9 Bottom surface crack patterns at failure of F2

Specimen F1 showed a little higher punching shear resistance than specimen F2 as shown in Table 2.

Table 2 Load capacity of test specimens

Footing ID	P_{exp} (kN)	P_{ACI} (kN)	P_{exp}/P_{ACI}
F1	450.20	92.62	4.86
F2	430.30	92.62	4.65

3.2 GFRP bar strains

Fig. 10, and Fig.11 show the longitudinal GFRP bar strain of specimens F1, and F2, respectively. Under a given load, tensile strain occurred in the specimen rebars because of the bending moment on the footing slab. In both figures, at maximum load, all the GFRP rebars did not reach their ultimate strain. This result indicates that both specimens did not fail in flexural failure mode.

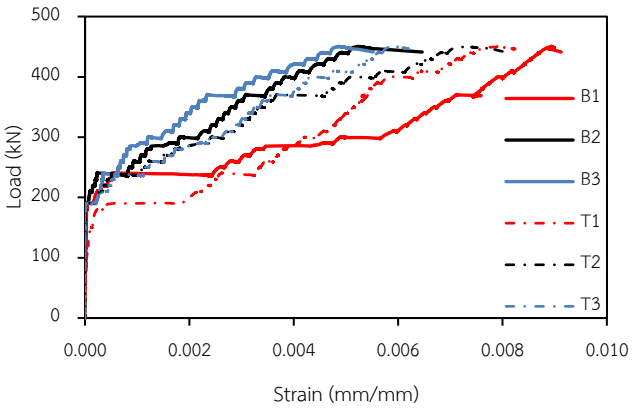

Fig. 10 Load-GFRP bars strain relationship of F1

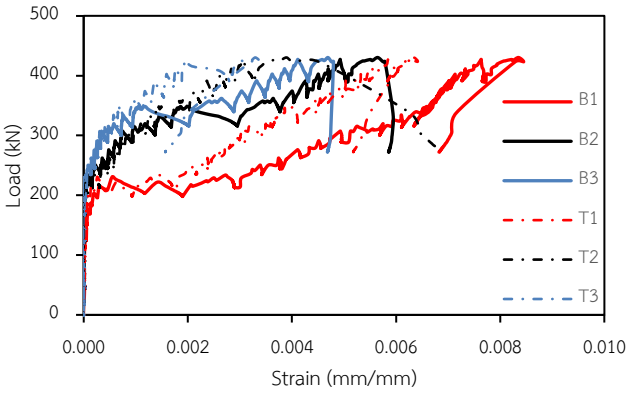

Fig. 11 Load-GFRP bars strain relationship of F2

3.3 Effect of different support types

Fig. 12 shows the experimentally measured load-displacement relationship with the reactions from nine springs.

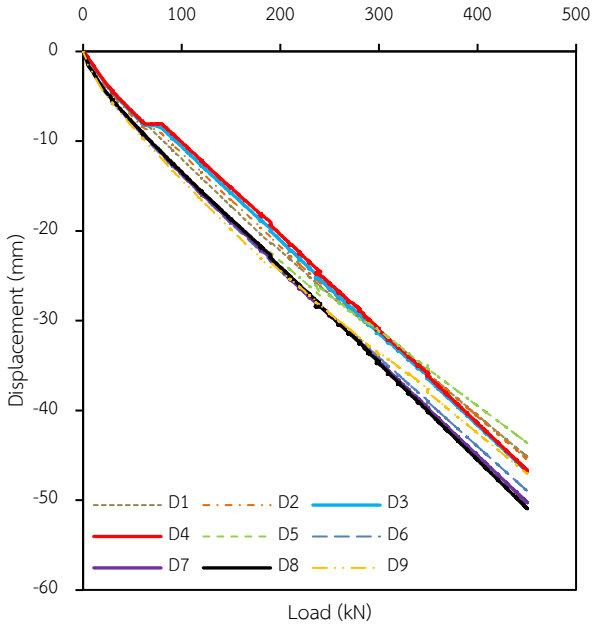

Fig. 12 Load-displacement relationship of F1

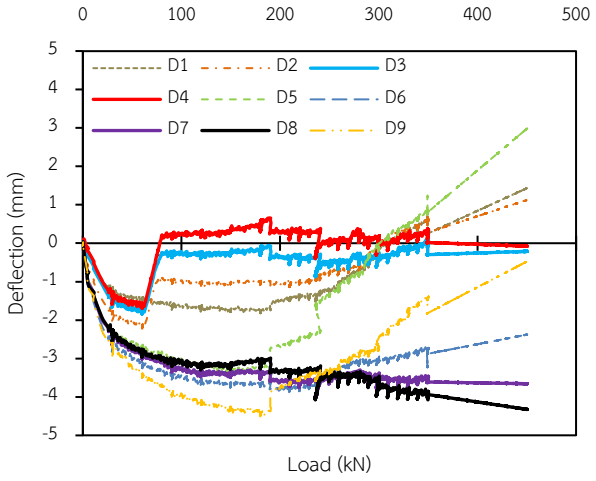

Fig. 13 Load-deflection relationship of F1

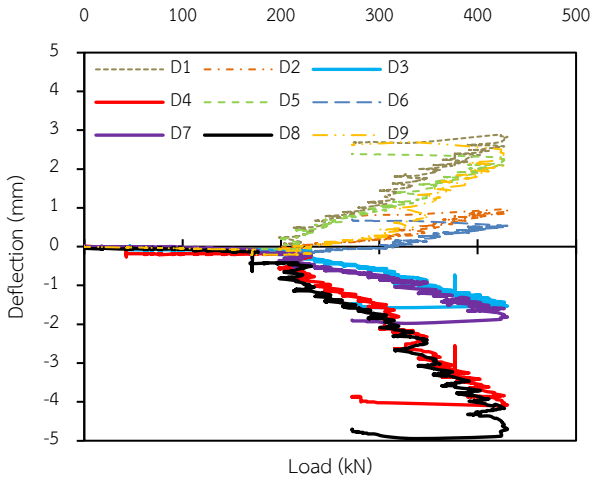

Fig. 14 Load-deflection relationship of F2

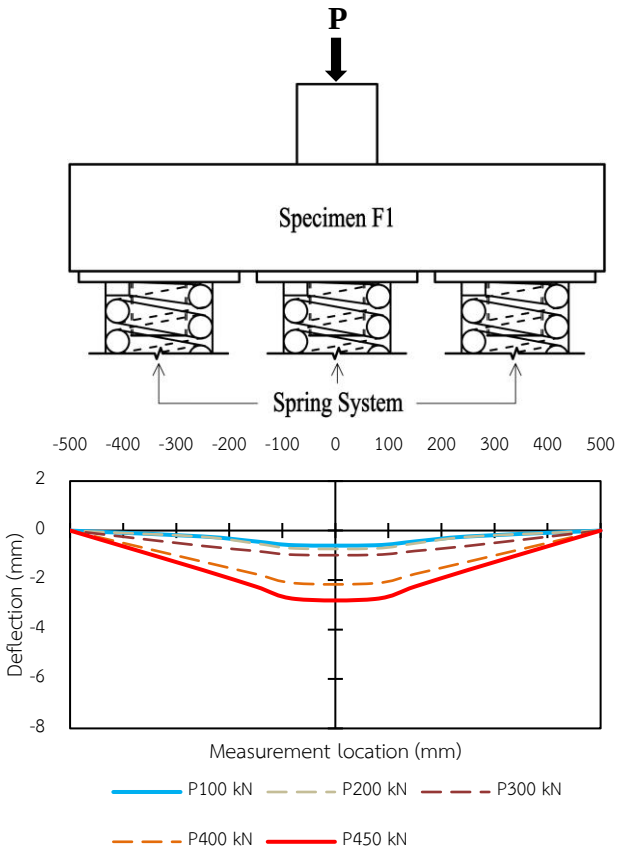

Fig. 15 Deflection of F1 in different stages of loading

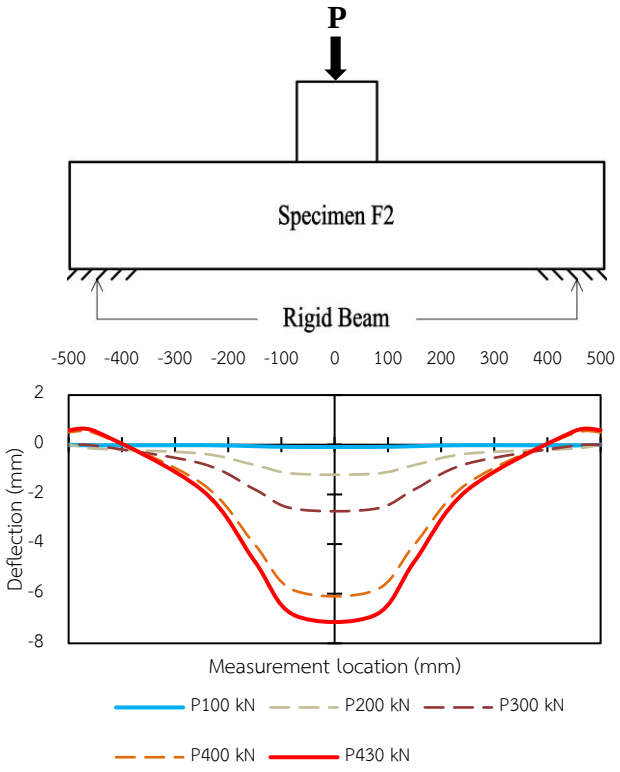

Fig. 16 Deflection of F2 in different stages of loading

The results obtained from Fig. 15 and Fig. 16 demonstrate that the foundation's stiffness significantly affects the footings' structural response. Specimen F1, which was supported by a bed of elastic springs, exhibited smaller structural deflection than specimen F2, which was supported by a rigid support. This can be corresponded to the fact that the rigid support allowed more movement of the footing, resulting in larger deflections under the applied loads. Both footing specimens initially experienced slight bending upon loading, but when they approached collapse, rapid deflection occurred.

4. Conclusions

Two full-scale reinforced concrete isolated footings reinforced with GFRP rebar specimens with the same structural dimensions and reinforcement ratio were tested to investigate the punching shear behavior of footings. The support types were examined. The results obtained from the experimental tests led to the following primary findings:

4.1 The elastic spring system remains consistent on its k value even when subjected to vertical settlement during the experiment, regardless of any different levels or confining factors.

4.2 Both specimens subjected to testing failed due to punching shear failure without showing any signs of one-way shear or flexural failures. There was no evidence of concrete crushing at the footing compression face at the column footing contact area, but instead of that, a brittle failure was observed with a sudden drop in the loaded area.

4.3 Specimen F1, supported by a bed of elastic springs showed wider cracks while specimen F2, supported by a rigid support showed larger structural deflection.

4.4 The maximum punching shear resistance for F1 specimen with an elastic spring system was greater than the ultimate capacity of F2 specimen with a rigid support by 4.62%.

4.5 The theoretically calculated value according to ACI CODE-440.11-22 [21] for punching shear resistance was 92.62 kN. The real value of punching shear resistance of specimens F1 and F2 according to tested results was 450.20 kN and 430.30 kN, respectively. In this case, the real resistance of specimens F1 and F2 was higher than the calculated value with 4.86 and 4.65 times, respectively. This means that ACI code is more reliable. The previous evidence supports that the punching shear resistance design based on the ACI code is extremely safe, possibly even more conservative.

Acknowledgment

The research received funding from the Sustainable Infrastructure Research and Development Center, Department of Civil Engineering, Faculty of Engineering at Khon Kaen University, as well as the Khon Kaen University Scholarship for ASEAN and GMS Countries' Personnel. The authors acknowledge GFRP KINGS Co., Ltd. for supplying the GFRP bars. The authors also would like to express their heartfelt appreciation to Mr. Poramin Sinthorn and the Full-Scale Lab team for their valuable contribution to the laboratory work.

References

[1] Sayan, S., Suraparb, K., and Chanachai, T. (2021). Flexural behavior of concrete beam reinforced with GFRP bars compared to concrete beam reinforced with conventional steel reinforcements. *Journal of Applied Science and Engineering* (Taiwan), 24(6), pp.883–890.

[2] Hatcher, D. S., Sozen, M. A., and Siess, C. P. (1969). Test of a Reinforced Concrete Flat Slab. *Journal of the Structural Division*, 95(6), pp.1051–1072.

[3] Lee, S. S., Moon, J., Park, K. S., and Bae, K. W. (2014). Strength of footing with punching shear preventers. *Scientific World Journal*, 2014. Article ID 474728, 15 pages.

[4] Hegger, J., Ricker, M., Ulke, B., and Ziegler, M. (2007). Investigations on the punching behaviour of reinforced concrete footings. *Engineering Structures*, 29(9), pp.2233–2241.

[5] Hegger, J., Ricker, M., and Sherif, A. G. (2009). Punching strength of reinforced concrete footings. *ACI Structural Journal*, 106(5), pp.706–716.

[6] Siburg, C., and Hegger, J. (2014). Experimental investigations on the punching behaviour of reinforced concrete footings with structural dimensions. *Structural Concrete*, 15(3), pp.331–339.

[7] Bonić, Z., and Folić, R. (2013). Punching of column footings - comparison of experimental and calculation results. *Građevinar*, 65(10), pp.887–899.

[8] Bonić, Z., Davidović, N., Vacev, T., Romić, N., Zlatanović, E., and Savić, J. (2017). Punching Behaviour of Reinforced Concrete Footings at Testing and According to Eurocode 2

and fib Model Code 2010. *International Journal of Concrete Structures and Materials*, 11(4), pp.657–676.

[9] Kivi, M. P., Araghi, H., and Oskouei, A. V. (2012). Investigation on GFRP Bar Performance in High Strength Concrete Footing. *Third Asia-Pacific Conference on FRP in Structures (APFIS2012)*, Hokkaido University Conference Hall, Sapporo, Japan, 2-4 February 2012, Article ID F1B02.

[10] Oskouei, A. V., Kivi, M. P., Araghi, H., and Bazli, M. (2017). Experimental study of the punching behavior of GFRP reinforced lightweight concrete footing. *Materials and Structures/Materiaux et Constructions*, 50(256), pp.1-14.

[11] Saleh, K. A., Said Hadad, H., and Nooman, M. T. (2022). PUNCHING SHEAR BEHAVIOR OF ISOLATED FOOTING REINFORCED WITH GLASS FIBER REINFORCED POLYMER BARS للقواعد المنفصلة المسلحة بأسياخ البوليمر المعزز القص اختراق سلوك الزجاجية بالألياف صالح أحمد خالد . , *Journal of Al-Azhar University Engineering Sector*, 17(62) . pp.218–189.

[12] Talbot, A. N. (1925). *Reinforced Concrete Wall Footings and Column Footings*. Bulletin No. 67, University of Illinois, USA.

[13] Lee, C., Lee, S., Ko, K., and Yang, J. M. (2017). Structural performance of SFRC slab-on-grade supported on elastic spring system. *Magazine of Concrete Research*, 69(15), pp.757–771.

[14] Truong, G. T., Choi, K. K., and Kim, H. S. (2017). Punching-shear behaviors of RC-column footings with various reinforcement and strengthening details. *Engineering Structures*, 151, pp.282–296.

[15] TIS.2973-2562. (2019). Fiber-reinforced polymers for non-prestressed concrete structures. *Thai Industrial Standards Institute (TISI)*.

[16] ASTM D7205/D7205M-06. (2016). Standard Test Method for Tensile Properties of Fiber Reinforced Polymer Matrix Composite Bars. *ASTM International*, West Conshohocken, PA, United States.

[17] TIS.24-2559. (2016). Steel bars for reinforced concrete: deformed bars. *Thai Industrial Standards Institute (TISI)*.

[18] TIS.20-2559. (2016). Steel bars for reinforced concrete: round bars. *Thai Industrial Standards Institute (TISI)*.

[19] ASTM C39/C39M-14. (2014). Standard Test Method for Compressive Strength of Cylindrical Concrete Specimens. *ASTM International*, West Conshohocken, PA, United States.

[20] Bowles, J.E. (1996). *Foundation and Analysis Design*. The McGraw-Hill Companies, Inc., pp.324.

[21] ACI CODE-440.11-22. Building Code Requirements for Structural Concrete Reinforced with Glass Fiber-Reinforced Polymer (GFRP) Bars—Code and Commentary. *ACI Committee 440*. Farmington Hills (USA): American Concrete Institute; 2022.